AD-A166 208 FAILURE PROPAGATION IN CONTINUUM MODELS OF LSS (LARGE SPACE STRUCTURES) PART 1(U) MASSACHUSETTS INST OF TECH CAMBRIDGE J H WILLIAMS ET AL. 01 NOV 85 1/1

UNCLASSIFIED AFOSR-TR-86-0094 F49620-85-C-0148 F/G 13/13 NL

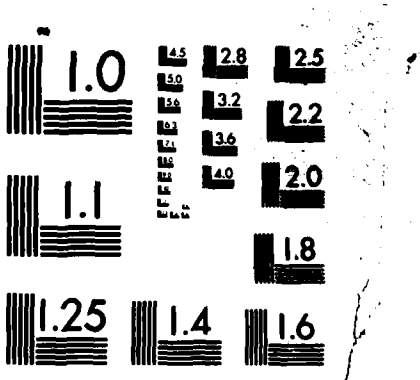

MICROCOPY RESOLUTION TEST CHART
NATIONAL BUREAU OF STANDARDS-1963-A

UNCLASSI

SECURITY CL

(2)

AD-A166 208

DOCUMENTATION PAGE

1a. REPORT Uncl	1b. RESTRICTIVE MARKINGS
2a. SECURITY CLASSIFICATION AUTHORITY	3. DISTRIBUTION/AVAILABILITY OF REPORT Approved for Public Release; Distribution Unlimited.
2b. DECLASSIFICATION/DOWNGRADING SCHEDULE	
4. PERFORMING ORGANIZATION REPORT NUMBER(S)	5. MONITORING ORGANIZATION REPORT NUMBER(S) AFOSR-TR- 86-0094
6a. NAME OF PERFORMING ORGANIZATION WEA	6b. OFFICE SYMBOL (If applicable)
6c. ADDRESS (City, State and ZIP Code) P.O. Box 260, MIT Branch Cambridge, MA 02139	7a. NAME OF MONITORING ORGANIZATION
	7b. ADDRESS (City, State and ZIP Code)
8a. NAME OF FUNDING/SPONSORING ORGANIZATION Air Force Office of Scientific Research	8b. OFFICE SYMBOL (If applicable) AFOSR/NA
8c. ADDRESS (City, State and ZIP Code) Bolling AFB, D.C. 20332	9. PROCUREMENT INSTRUMENT IDENTIFICATION NUMBER F49620-85-C-0148

DTIC ELECTE APR 0 1 1986 S D

10. SOURCE OF FUNDING NOS.			
PROGRAM ELEMENT NO.	PROJECT NO.	TASK NO.	WORK UNIT NO.
61102F	2302	B1	

11. TITLE (Include Security Classification) Failure Propagation in Continuum Models of LSS, Part I (Unclassified)

12. PERSONAL AUTHOR(S) James H. Williams, Jr. and Samson S. Lee

13a. TYPE OF REPORT	13b. TIME COVERED	14. DATE OF REPORT (Yr., Mo., Day)	15. PAGE COUNT
Technical	FROM 1 Sept 85 TO 1 Nov 85	85, November, 1	30

16. SUPPLEMENTARY NOTATION

17 COSATI CODES		
FIELD	GROUP	SUB. GR.

18. SUBJECT TERMS (Continue on reverse if necessary and identify by block number)
Wave Propagation
Dynamic Failure
Lattice Structures
Large Space Structures

19. ABSTRACT (Continue on reverse if necessary and identify by block number)

Large space structures (LSS) can often be modelled adequately as equivalent anisotropic continua. In this study concepts in failure mechanics and wave propagation are applied to analyze the dynamic failure (fracture, buckling, joint disassembly, etc.) and failure arrest behavior of such an equivalent continuum. For simplicity, the equivalent continuum is assumed to be orthotropic. Furthermore, the transverse shear deformation of the equivalent continuum is assumed to dominate.

Double cantilever beam models are well established fracture mechanics models in the study of crack propagation in a continuum. An orthotropic double cantilever shear beam (DCSB) model is adopted here to study Mode I dynamic failure (which for convenience is assumed to be fracture) and arrest in continuum models of lattice structures. The orthotropic DCSB model consists of both a primary material and a finite width arrester section. The DCSB model has predicted that under the proper conditions the crack may arrest.

20. DISTRIBUTION/AVAILABILITY OF ABSTRACT	21. ABSTRACT SECURITY CLASSIFICATION
UNCLASSIFIED/UNLIMITED ☒ SAME AS RPT. ☐ DTIC USERS ☐	Unclassified

22a. NAME OF RESPONSIBLE INDIVIDUAL	22b. TELEPHONE NUMBER (Include Area Code)	22c. OFFICE SYMBOL
Anthony K. Amos	202/767-4937	AFOSR/NA

DD FORM 1473, 83 APR EDITION OF 1 JAN 73 IS OBSOLETE.

UNCLASSIFIED
SECURITY CLASSIFICATION OF THIS PAGE

DTIC FILE COPY

19. ABSTRACT (Continued)

when any of the following conditions is satisfied:

1) When the initial reflected disturbance catches the crack tip, before the crack tip reaches the arrester section;

2) When the crack tip enters the arrester section;

3) When the crack tip exits the arrester section; or

4) When the initial reflected disturbance catches the crack tip, after the crack tip has exited from the arrester section.

It is shown that condition (1) is absolute, meaning that the crack is always arrested. Achieving conditions (2), (3) and (4) may or may not result in crack arrest. Condition (3) is independent of either conditions (2) or (4), and condition (4) is a less stringent condition (that is, easier to satisfy the arrest criterion) than condition (2).

A major assumption in this study is that the failure can be described by a "failure toughness" that is independent of the velocity of failure propagation. Also, it is emphasized that while the specific failure mode discussed here is fracture, this particular selection of a failure mode is done only for illustrative specificity. In fact, as indicated above, the "failure" could represent buckling of individual elements, loss of joint integrity, rupture or any other energy-absorbing degradation process in a large space lattice structure.

ACKNOWLEDGMENTS

The Air Force Office of Scientific Research (Project Monitor, Dr. Anthony K. Amos) is gratefully acknowledged for its support of this research.

NOTICE

This document was prepared under the sponsorship of the Air Force. Neither the US Government nor any person acting on behalf of the US Government assumes any liability resulting from the use of the information contained in this document. This notice is intended to cover WEA as well.

Accesion For	
NTIS CRA&I	☒
DTIC TAB	☐
Unannounced	☐
Justification	
By	
Distribution /	
Availability Codes	
Dist	Avail and / or Special
A-1	

INTRODUCTION

Space stations, satellite solar power stations, space communication antennas, and space platforms are examples of orbiting large space structures proposed both for military and nonmilitary applications [1]. An attractive design for large space structures is the construction of structures with a large number of repetitive lattice elements. However, the static and dynamic analyses of large lattice structures using conventional methods are cumbersome because of the large number of structural elements involved. Thus, methods have been devised such that large space structures may be modelled adequately as equivalent anisotropic continua [2-4].

The dynamic failure (fracture, buckling, joint disassembly, etc.) propagation and failure arrest behaviors of an equivalent continuum model of space lattice structures will be considered in this study using concepts in fracture mechanics and wave propagation. For simplicity, the equivalent continuum will be assumed to be orthotropic. Furthermore, the transverse shear deformation of the equivalent continuum will be assumed to dominate. The geometry and material of the basic repetitive lattice structure are such that the structure can be modelled as an orthotropic shear continuum.

Double cantilever beam models are well established fracture mechanics models in the study of crack propagation in a material continuum [5]. An orthotropic double cantilever shear beam (DCSB) model will be used here to study Mode I dynamic failure (which for convenience is assumed to be

fracture) and arrest in continuum models of lattice structures. Orthotropic DCSB models have been used to study crack propagation in composite materials [6,7] and the results can be applied directly to continuum models of lattice structures.

The fracture behavior of a continuum is characterized by the dynamic fracture toughness which is the incremental energy absorbed by the incremental crack extension. It is shown that for a velocity-independent dynamic fracture toughness, the crack-tip speed is constant and the crack is arrested abruptly when the reflected initial disturbance catches the crack tip in an orthotropic homogeneous DCSB model [6]. When a second material region of semi-infinite width is introduced as a crack arrester section, it is observed that with the proper choice of arrester materials, the crack can be stopped at the materials interface [7]. Furthermore, if the crack is not stopped at the interface, the crack propagates in the arrester section with a different constant velocity and the crack can then be stopped when the reflected initial disturbance catches the crack tip. It is important to note, however, that the introduction of the arrester section may actually degrade the structure if the crack is not arrested at this point [7]. (The orthotropic DCSB mdoel containing a semi-infinite width arrester region is denoted as the orthotropic duplex DCSB model [7].)

In this study, an orthotropic DCSB model with a finite width arrester section will be considered. The effect of the finite width arrester section on crack propagation will be studied. In a specific

space lattice structure, the finite width arrester section might represent a local region in the lattice structure where a different repetitive lattice truss, a joint, a material change occurs. The continuum model representing the primary space lattice structure will be denoted as the primary material and the continuum model of the localized different region will be denoted as the arrester material.

Again, it should be emphasized that while the specific failure mode discussed here is fracture, this is done only for convenience and specificity. In fact, as already indicated, the "failure" could represent buckling collapse of individual elements, loss of joint integrity, fracture or any other energy-absorbing degradation process in the lattice structure.

DCSB WITH FINITE WIDTH ARRESTER SECTION

The structure to be analyzed consists of a primary material and a finite width arrester section as shown in Fig. 1. The arms of the cracked specimen are assumed to be shear beams. Thus, the shear beams exist in the region $0 < x < \ell(t)$, where x is the coordinate in the direction of crack propagation, t is time, and $\ell(t)$ is the time-dependent crack length. The transverse displacement in each arm is denoted by $w(x,t)$. The specimen initially contains a crack of length ℓ_0. The crack opening at $x = 0$ is maintained constant at $2w_0$ throughout the test. The primary material has shear modulus G_1, mass density ρ_1, and a shear wave speed given by

$$C_1 = \sqrt{\frac{G_1}{\rho_1}} \quad . \tag{1}$$

The material in the arrester section has shear modulus G_2, mass density ρ_2, and a shear wave speed given by

$$C_2 = \sqrt{\frac{G_2}{\rho_2}} \quad . \tag{2}$$

The arrester strip is located at a distance ℓ_{p_1}, which in order to encounter the moving crack tip must satisfy eqn. (3) of [7],

$$\ell_{p_1} < n\ell_0 \tag{3}$$

where n is the bluntness parameter. From the duplex specimen result [7], it is known that at the primary material/arrester material interface the

crack may arrest with an arrest length ℓ_{p_1}. If arrest does not occur at ℓ_{p_1}, the crack may arrest later when the initial disturbance catches the crack tip with a corresponding arrest length ℓ_c as given in eqn. (51) of [7] as

$$\ell_c = \ell_{p_1}\left(\frac{n+1}{n-1}\right)\left(\frac{1-\frac{\dot{\ell}_1}{c_1}}{1-\frac{\dot{\ell}_2}{c_2}}\right) + \ell_0\left[\frac{2}{1-\frac{\dot{\ell}_2}{c_2}} - 1\right] \tag{4}$$

where $\dot{\ell}_1$ and $\dot{\ell}_2$ are the crack speeds in the primary and arrester sections, respectively. For the finite width arrester section problem, it will be assumed that the arrester strip extends from ℓ_{p_1} and includes the region up to ℓ_{p_2} which is less than ℓ_c. Thus,

$$\ell_{p_1} < \ell_{p_2} < \ell_c \quad . \tag{5}$$

The boundary conditions and the initial conditions in terms of the slope q and transverse velocity v are the same as those derived in [6]. The boundary conditions are

$$v = 0 \qquad \text{at } x = 0 \tag{6}$$

$$q\dot{\ell} + v = 0 \qquad \text{at } x = \ell(t) \tag{7}$$

where v is the transverse velocity $(\partial w/\partial t)$ and q is the slope $(\partial w/\partial x)$. The initial conditions are

$$v = 0 \tag{8}$$

$$q = q_0 = -\frac{w_0}{\ell_0} \quad . \tag{9}$$

In addition, there are continuity matching conditions at the primary ma-

terial/arrester material interface and subsequently at the arrester material/primary material interface. The equilibrium requirement on the shear force across the interface may be expressed as

$$(Gq)_- = (Gq)_+ \tag{10}$$

and the geometric compatibility requirement on the transverse velocity across the interface may be expressed as

$$v_- = v_+ \tag{11}$$

where the minus (-) subscript is used to denote the material just to the left of the interface and the plus (+) subscript is used to denote the material just to the right of the interface.

In an earlier paper [6], it was shown that in the orthotropic shear beam disturbances propagate along characteristics, along which the following equations hold:

$$C_s q - v = \text{Constant} \qquad \text{along } \frac{dx}{dt} = C_s \tag{12}$$

$$C_s q + v = \text{Constant} \qquad \text{along } \frac{dx}{dt} = -C_s \tag{13}$$

where C_s is the shear wave speed of the material.

CRACK PROPAGATION AND ARREST CRITERIA

The dynamic fracture criteria are [7]

$$\mathcal{G}_d = R_i \qquad i = 1,2 \tag{14}$$

and the fracture arrest criteria are [7]

$$\mathcal{G}_d < R_i \qquad i = 1,2 \tag{15}$$

where $\mathcal{G}_d$ is the dynamic crack extension force and R is the dynamic fracture toughness, both per unit of beam width. The dynamic fracture toughness of the primary material and the arrester material are denoted by R_1 and R_2, respectively. Both R_1 and R_2 are assumed to be independent of the crack-tip speed. The dynamic crack extension force is [7]

$$\mathcal{G}_d = G_i h \left(1 - \frac{\dot{\ell}^2}{C_i^2}\right) q^2(\ell,t) \qquad i = 1,2 \quad . \tag{16}$$

By setting $\dot{\ell} = 0$ in eqn. (16) and by using eqn. (14), the minimum crack-tip slope q_{min} that is required to maintain crack propagation is [6]

$$q_{min(i)} = \sqrt{\frac{R_i}{G_i h}} \qquad i = 1,2 \quad . \tag{17}$$

An equivalent fracture arrest criterion is

$$\max q < q_{min(i)} \qquad i=1,2 \quad . \tag{18}$$

where max q is the maximum crack-tip slope.

MOTION OF DCSB DURING CRACK PROPAGATION

At time $t = 0$, the crack tip begins to propagate in the x direction. The motion of the crack tip and the specimen arms may be described in terms of the (x,t) plane as shown in Fig. 2. As the crack begins to extend, initial disturbances in the values of $v(x,t)$ and $q(x,t)$ are propagated along line AB. At point B, these disturbances reflect from the left-hand boundary $x = 0$ and then propagate back along line BC through the arrester section. Disturbances may then reflect from the moving crack tip at point C and propagate back toward the left-hand boundary. Also, as the crack tip moves through the materials interfaces at points H and S, disturbances are propagated toward the left-hand boundary. Reflections at points such as P, Q, and R on the interfaces can be traced in a similar manner.

In this simplified shear beam model, the finite size of the arrester section has no effect on crack propagation if the crack length $\ell(t)$ is less than ℓ_{p_2}. Thus, the results from the duplex specimen analysis [7] are valid up to point S.

Crack Motion Just Beyond Point S

At any location in the (x,t) plane, the values of $v(x,t)$ and $q(x,t)$ may be determined by following eqns. (12) and (13) along the characteristics. The primary focus of this analysis is the behavior of the dynamic crack extension force beyond point S. Because the dynamic crack extension

depends on the crack-tip parameters, namely, the slope and the velocity, the calculations which follow will be directed toward the determination of these details at the crack tip.

In order to determine the conditions along the crack-tip trajectory beyond point S, the technique used in [7] to obtain crack-tip properties just beyond point H will be applied. In Fig. 2 consider point 22 which is infinitesimally beyond point S and is on the crack tip. Also, consider point 21 which is infinitesimally close to point 22 but which is on the arrester material side of the interface. Because points 21 and 22 are infinitesimally close but on different sides of the materials interface, the matching conditions in eqns. (10) and (11) may be assumed to hold between them. Similarly, points 4 and 5 represent the "same" location on the left-hand materials interface except that point 4 is in the primary material and point 5 is in the arrester material.

Considering Fig. 2, the characteristic eqns. (12) and (13) yield

$$C_2 q_5 - v_5 = C_2 q_{21} - v_{21} \tag{19}$$

$$C_2 q_5 + v_5 = C_2 q_2 + v_2 \tag{20}$$

$$C_1 q_3 - v_3 = C_1 q_4 - v_4 \ . \tag{21}$$

Point 3 is below the initial disturbance line AB and is therefore in the initial state as described by eqns. (8) and (9),

$$v_3 = 0 \tag{22}$$

$$q_3 = q_0 \ . \tag{23}$$

Point 22 is on the crack tip, so the boundary condition in eqn. (7) gives

$$q_{22}\dot{\ell}_{22} + v_{22} = 0 \quad . \tag{24}$$

The matching conditions (10) and (11) between points 21 and 22 are

$$G_2 q_{21} = G_1 q_{22} \tag{25}$$

$$v_{21} = v_{22} \tag{26}$$

and the matching conditions (10) and (11) between points 4 and 5 are

$$G_1 q_4 = G_2 q_5 \tag{27}$$

$$v_4 = v_5 \quad . \tag{28}$$

The state at point 2 is given by eqns. (24) and (25) of [7] as

$$q_2 = \frac{q_0}{\left(\frac{G_2}{G_1} + \frac{\dot{\ell}_2}{C_1}\right)} \tag{29}$$

$$v_2 = -\frac{\dot{\ell}_2 q_0}{\left(\frac{G_2}{G_1} + \frac{\dot{\ell}_2}{C_1}\right)} \quad . \tag{30}$$

As shown in Appendix A, eqns. (19) through (30) may be solved to give

$$q_{22} = q_0 \left[\frac{\dfrac{\left(1 - \dfrac{C_1}{C_2}\dfrac{G_2}{G_1}\right)}{\left(\dfrac{G_2}{G_1} + \dfrac{\dot{\ell}_2}{C_1}\right)}\left(1 - \dfrac{\dot{\ell}_2}{C_2}\right) + 2\dfrac{C_1}{C_2}}{\left(1 + \dfrac{C_1}{C_2}\dfrac{G_2}{G_1}\right)\left(\dfrac{G_1}{G_2} + \dfrac{\dot{\ell}_{22}}{C_2}\right)} \right] \tag{31}$$

$$v_{22} = -\dot{\ell}_{22} q_{22} \tag{32}$$

where $\dot{\ell}_2$ is given by eqn. (31) of [7]. The crack speed at point 22 is

$\dot{\ell}_{22}$ which as shown in [7] may be determined from eqns. (14) and (16). The value of $\dot{\ell}_{22}$ will not be computed, however, since only the crack arrest conditions at point S are sought in this study.

Crack Arrest Conditions at Point S

The crack arrest criterion in terms of the crack-tip slope as given by eqn. (18) will now be used. The minimum crack-tip slope required to maintain a propagating crack in the primary material beyond point S will be given by eqn. (17) as

$$q_{min(1)} = \sqrt{\frac{R_1}{G_1 h}} \quad . \tag{33}$$

The maximum available crack-tip slope at a point, such as point 22, just beyond point S is obtained for quasi-static crack extension ($\dot{\ell}_{22} \approx 0$) from eqn. (31) as

$$\max q_{22} = q_0 \left[\frac{\left(1 - \frac{C_1}{C_2}\frac{G_2}{G_1}\right)\left(1 - \frac{\dot{\ell}_2}{C_2}\right) + 2\frac{C_1}{C_2}}{\left(\frac{G_2}{G_1} + \frac{\dot{\ell}_2}{C_1}\right)} \Bigg/ \frac{G_1}{G_2}\left(1 + \frac{C_1}{C_2}\frac{G_2}{G_1}\right) \right] \quad . \tag{34}$$

Because point 22 is just beyond point S, according to eqn. (18) crack arrest at point S requires

$$q_{min(1)} > \max q_{22} \quad . \tag{35}$$

Substitution of eqns. (33) and (34) into eqn. (35) gives

$$\sqrt{\frac{R_1}{G_1 h}} > q_0 \left[\frac{\left(1 - \frac{C_1}{C_2}\frac{G_2}{G_1}\right)\left(1 - \frac{\dot{\ell}_2}{C_2}\right) + 2\frac{C_1}{C_2}}{\left(\frac{G_2}{G_1} + \frac{\dot{\ell}_2}{C_1}\right)\frac{G_1}{G_2}\left(1 + \frac{C_1}{C_2}\frac{G_2}{G_1}\right)} \right] . \tag{36}$$

Substitution of q_0 as given by eqn. (30) of [6] into eqn. (36) gives

$$1 > \sqrt{n}\left[\frac{\left(1 - \frac{C_1}{C_2}\frac{G_2}{G_1}\right)\left(1 - \frac{\dot{\ell}_2}{C_2}\right) + 2\frac{C_1}{C_2}}{\left(\frac{G_2}{G_1} + \frac{\dot{\ell}_2}{C_1}\right)\frac{G_1}{G_2}\left(1 + \frac{C_1}{C_2}\frac{G_2}{G_1}\right)} \right] \tag{37}$$

where as indicated earlier $\dot{\ell}_2$ is given by eqn. (31) of [7]. Eqn. (37) is the crack arrest criterion at point S. If eqn. (37) is satisfied, the crack will arrest abruptly as the crack tip emerges from the arrester section.

For the specimen shown in Fig. 1, the results from the duplex specimen analysis [7] hold until the crack tip reaches the right-hand boundary of the arrester section at point S. The duplex specimen analysis shows that the crack may be arrested at the left-hand boundary of the arrester section. This arrest condition is given by eqn. (32) of [7]. As shown in Appendix B, this arrest condition can be simplified to

$$n \frac{G_1 R_1}{G_2 R_2} < 1 \quad . \tag{38}$$

An alternate approach using eqn. (18) in terms of the crack-tip slope has also been performed in Appendix B to yield the same result. Eqn. (38) is the condition for crack arrest at point H.

Eqn. (37) is the crack arrest condition at point S. Eqns. (37) and (38) are independent because eqn. (38) does not contain the shear wave speeds whereas eqn. (37) contains the shear wave speeds as well as the relatively complicated $\dot{\ell}_2$. Thus, it is possible to design an arrester strip system to arrest a crack when it enters the arrester by considering eqn. (38) or when it exits the arrester section by considering eqn. (37). Therefore, the finite width arrester section gives an additional independent opportunity to arrest the crack before the reflected initial disturbance catches the crack tip at point C. As a further remark, it is interesting to note that whereas the crack arrest conditions at points H and S are independent, it is shown in Appendix C from the results of [7] that the crack arrest condition at point C is always easier to satisfy than the arrest condition at point H.

If the crack is arrested at point S, the crack arrest length is

$$\ell_S = \ell_{P_2} \quad . \tag{39}$$

The crack arrest time is

$$t_S = t_H + \frac{\left(\ell_{P_2} - \ell_{P_1}\right)}{\dot{\ell}_2} \quad . \tag{40}$$

Replacing t_H in eqn. (40) by the value given in eqn. (34) of [7] gives

$$t_s = \frac{\ell_{p_1}}{c_1}\left(\frac{n+1}{n-1}\right) + \frac{\left(\ell_{p_2} - \ell_{p_1}\right)}{\dot{\ell}_2} \quad . \tag{41}$$

Eqns. (39) and (41) give the crack arrest length and time, respectively.

CONCLUSIONS

Large space structures can often be modelled adequately as equivalent anisotropic continua. In this study concepts in failure mechanics and wave propagation have been applied to analyze the dynamic failure and failure arrest behavior of such an equivalent continuum. For specificity, fracture is analyzed as the failure process, although buckling, the loss of joint integrity or any energy-absorbing degradation process in the lattice could have been considered.

An orthotropic double cantilever shear beam (DCSB) model has been analyzed to study Mode I dynamic fracture and arrest in continuum models of lattice structures. The DCSB model consists of both a primary material and a finite width arrester section. For the DCSB model consisting of orthotropic materials having a crack-speed-independent dynamic fracture toughness, the DCSB model predicts that under the proper conditions the crack may arrest abruptly as it enters the arrester region [7]. Further, if the arrester has a finite width, the crack may arrest as it exits the arrester region. The arrest condition at the exit of the arrester region has been derived here and it is noted that this condition is independent of the other arrest conditions. Also, the arrest conditions at the entrance of the arrester region and at the point at which the initial reflected disturbance overtakes the crack tip are compared. It has been shown that the latter arrest condition is a less stringent condition than the former, indicating that if the crack is not arrested at the

entrance of the arrester region, the crack may be arrested when the initial reflected disturbance overtakes the crack tip beyond the arrester section.

The results in this study have provided an analytical basis for the investigation of dynamic failure propagation and failure arrest in space lattice structures by applying fracture mechanics and wave propagation techniques to an equivalent continuum material model of the space lattice structure.

REFERENCES

[1] M.F. Card and W.J. Boyer, "Large Space Structures---Fantasies and Facts", Proceedings of AIAA/ASME/ASCE/AHS 21st Structures, Structural Dynamics and Materials Conference, Held in Seattle, WA, May 12-14, 1980, Part 1, American Institute of Aeronautics and Astronautics, N.Y., NY, 1980, pp. 101-114.

[2] A.K. Noor, "Assessment of Current State of the Art in Modeling Techniques and Analysis Methods for Large Space Structures", Modeling, Analysis, and Optimization Issues for Large Space Structures, NASA Conference Publication 2258, Proceedings of a Workshop held in Williamsburg, VA, May 13-14, 1982, National Aeronautics and Space Administration, Washington, D.C., 1983, pp. 5-32.

[3] A.K. Noor, M.S. Anderson, and W.H. Greene, "Continuum Models for Beam- and Platelike Lattice Structures", AIAA Journal, Vol. 16, No. 2, December 1978, pp. 1219-1228.

[4] C.T. Sun, B.J. Kim, and J.L. Bogdanoff, "On the Derivation of Equivalent Simple Models for Beam- and Plate-Like Structures in Dynamic Analysis", Proceedings of AIAA/ASME/ASCE/AHS 22nd Structures, Structural Dynamics and Materials Conference and AIAA Dynamics Specialists Conference, Held in Atlanta, GA, April 6-8, 1981, Part 2, American Institute of Aeronautics and Astronautics, N.Y., NY 1981, pp. 523-532.

[5] L.B. Freund, "A Simple Model of the Double Cantilever Beam Crack Propagation Specimen", Journal of the Mechanics and Physics of Solids", Vol. 25, No. 1, February 1977, pp. 69-79.

[6] S.S. Lee, J.H. Williams, Jr., and P.N. Kousiounelos, "Double Cantilever Shear Beam Model of Dynamic Fracture in Unidirectional Fibre Composites", Fibre Science and Technology, Vol. 17, No. 2, September 1982, pp. 99-122.

[7] J.H. Williams, Jr., and S.S. Lee, "Double Cantilever Shear Beam Model of Dynamic Fracture in Duplex Fiber Composites", International Journal of Fracture, Vol. 19, No. 1, May 1982, pp. 3-16.

APPENDIX A: CRACK-TIP VELOCITY AND SLOPE JUST BEYOND POINT S

Eqns. (19) through (30) can be solved to obtain the crack-tip velocity and slope at point 22. Substitution of eqns. (22) and (23) into eqn. (21) gives

$$C_1 q_0 = C_1 q_4 - v_4 \quad . \tag{A1}$$

Substitution of eqns. (27) and (28) into eqn. (A1) gives

$$C_1 q_0 = C_1 \frac{G_2}{G_1} q_5 - v_5 \quad . \tag{A2}$$

Addition of eqns. (20) and (A2) and rearrangement of their sum give

$$q_5 = \frac{1}{\left(C_2 + C_1 \frac{G_2}{G_1}\right)} (C_2 q_2 + v_2 + C_1 q_0) \quad . \tag{A3}$$

Substitution of eqn. (A3) into eqn. (20) gives

$$v_5 = C_2 q_2 + v_2 - \frac{1}{\left(1 + \frac{C_1}{C_2}\frac{G_2}{G_1}\right)} (C_2 q_2 + v_2 + C_1 q_0) \quad . \tag{A4}$$

Replacing v_{22} in eqn. (26) by the use of eqn. (24) yields

$$v_{21} = -q_{22} \dot{\ell}_{22} \quad . \tag{A5}$$

Substitution of eqns. (25) and (A5) into eqn. (19) gives

$$C_2 q_5 - v_5 = q_{22} \left(C_2 \frac{G_1}{G_2} + \dot{\ell}_{22}\right) \quad . \tag{A6}$$

Substitution of eqns. (A3) and (A4) into eqn. (A6) and solving for q_{22} give

$$q_{22} = \frac{\left(1 - \frac{C_1}{C_2}\frac{G_2}{G_1}\right)(C_2 q_2 + v_2) + 2C_1 q_0}{\left(1 + \frac{C_1}{C_2}\frac{G_2}{G_1}\right)\left(C_2\frac{G_1}{G_2} + \dot{\ell}_{22}\right)} \quad . \tag{A7}$$

Eliminating q_2 via eqn. (29) and v_2 via eqn. (30) in eqn. (A7) yields

$$q_{22} = q_0\left[\frac{\frac{\left(1 - \frac{C_1}{C_2}\frac{G_2}{G_1}\right)}{\left(\frac{G_2}{G_1} + \frac{\dot{\ell}_2}{C_1}\right)}\left(1 - \frac{\dot{\ell}_2}{C_2}\right) + 2\frac{C_1}{C_2}}{\left(1 + \frac{C_1}{C_2}\frac{G_2}{G_1}\right)\left(\frac{G_1}{G_2} + \frac{\dot{\ell}_{22}}{C_2}\right)}\right] . \tag{A8}$$

Also, from eqn. (32)

$$v_{22} = -\dot{\ell}_{22} q_{22} \quad . \tag{A9}$$

Eqns. (A8) and (A9) describe the crack-tip slope and velocity, respectively, at point 22, which is a point on the crack tip just beyond point S.

APPENDIX B: CRACK ARREST CRITERION AT POINT H

The crack arrest criterion at point H is given in eqn. (32) of [7] as

$$\frac{\rho_1}{\rho_2} - \frac{G_2}{G_1} + n\frac{R_1}{R_2} - \frac{1}{n}\frac{G_2\rho_1 R_2}{G_1\rho_2 R_1} < 0 \quad . \tag{B1}$$

Eqn. (B1) can be manipulated to give

$$\left(\frac{1}{n}\frac{\rho_1 R_2}{\rho_2 R_1} + 1\right)\left(n\frac{G_1 R_1}{G_2 R_2} - 1\right) < 0 \quad . \tag{B2}$$

Because the terms in the first set of parentheses on the left-hand side of eqn. (B2) are always positive, the satisfaction of the inequality (B2) requires that

$$n\frac{G_1 R_1}{G_2 R_2} < 1 \quad . \tag{B3}$$

Thus, expression (B1) can be simplified to expression (B3).

Eqn. (B1) was obtained by setting $\dot{\ell}_2 \leq 0$ after using the fracture criterion in eqn. (14) and the crack driving force in eqn. (16). An alternate method is to consider the crack-tip slope and to use eqn. (18) to derive the crack arrest conditions. The minimum crack-tip slope required to maintain a propagating crack in the arrester material is given by eqn. (17) as

$$q_{min(2)} = \sqrt{\frac{R_2}{G_2 h}} \quad . \tag{B4}$$

The maximum available crack-tip slope at a point just beyond point H,

such as point 2 in Fig. 3 of [7], is obtained for quasi-static crack extension ($\dot{\ell}_2 \approx 0$) from eqn. (24) in [7] as

$$\max q_2 = \frac{G_1}{G_2} q_0 \quad . \tag{B5}$$

Because point 2 is just beyond point H, for crack arrest at point H eqn. (18) requires that

$$q_{\min(2)} > \max q_2 \quad . \tag{B6}$$

Substitution of eqns. (B4) and (B5) into eqn. (B6) gives

$$\sqrt{\frac{R_2}{G_2 h}} > \frac{G_1}{G_2} q_0 \quad . \tag{B7}$$

Replacing q_0 by eqn. (30) of [1], eqn. (B7) becomes

$$1 > n \frac{G_1 R_1}{G_2 R_2} \quad . \tag{B8}$$

Eqn. (B8) is identical to eqn. (B3) as expected. As a check, by setting $G_1 = G_2$ and $R_1 = R_2$ eqn. (B3) or eqn. (B8) indicates that the crack will not arrest because $1 \not> n$. Recall that in accordance with [6], if there is no arrester section, the crack will not arrest until the crack tip reaches point C, the point at which the reflected initial disturbance catches the crack tip. Finally, it is interesting to note that the materials' densities, and thus the shear wave speeds, do not affect the crack arrest criterion.

APPENDIX C: COMPARISON OF CRACK ARREST CRITERIA AT POINTS H AND C

The crack arrest condition at point H as the crack tip enters the arrester section is given in eqn. (38) as

$$1 > n \frac{G_1 R_1}{G_2 R_2} \quad . \tag{C1}$$

Also, in a duplex specimen, the crack arrest condition at point C is given in eqn. (67) of [7] as

$$\sqrt{\frac{R_2}{G_2}} > \sqrt{\frac{nR_1}{G_1}} \left[\frac{\frac{2}{n}\frac{G_1}{G_2} + \frac{\left(1 - \frac{\dot{\ell}_2}{C_2}\right)\left(\frac{C_2}{C_1}\frac{G_1}{G_2} - 1\right)}{\left(\frac{G_2}{G_1} + \frac{\dot{\ell}_2}{C_1}\right)}}{\left(\frac{C_2}{C_1}\frac{G_1}{G_2} + 1\right)} \right] \quad . \tag{C2}$$

Eqn. (C2) can be manipulated as follows:

$$\left(\frac{C_2}{C_1}\frac{G_1}{G_2} + 1\right)\sqrt{\frac{R_2}{G_2}} > \sqrt{\frac{nR_1}{G_1}} \left[\frac{2}{n}\frac{G_1}{G_2} + \frac{\left(1 - \frac{\dot{\ell}_2}{C_2}\right)\left(\frac{C_2}{C_1}\frac{G_1}{G_2} - 1\right)}{\left(\frac{G_2}{G_1} + \frac{\dot{\ell}_2}{C_1}\right)} \right] ,$$

$$\left(\frac{C_2}{C_1}\frac{G_1}{G_2} + 1\right) > \sqrt{n\frac{R_1 G_1}{R_2 G_2}}\,\frac{G_2}{G_1} \left[\frac{2}{n}\frac{G_1}{G_2} + \frac{\left(1 - \frac{\dot{\ell}_2}{C_2}\right)\left(\frac{C_2}{C_1}\frac{G_1}{G_2} - 1\right)}{\left(\frac{G_2}{G_1} + \frac{\dot{\ell}_2}{C_1}\right)} \right] ,$$

or,

$$\frac{1}{\sqrt{n\,\frac{G_1R_1}{G_2R_2}}} > \frac{\left[\frac{2}{n} + \frac{\left(1 - \frac{\dot{\ell}_2}{C_2}\right)\left(\frac{C_2}{C_1}\frac{G_1}{G_2} - 1\right)}{\left(1 + \frac{G_1}{G_2}\frac{\dot{\ell}_2}{C_1}\right)}\right]}{\left(\frac{C_2}{C_1}\frac{G_1}{G_2} + 1\right)} \quad . \tag{C3}$$

Eqn. (C1) may be rewritten as

$$\frac{1}{\sqrt{n\,\frac{G_1R_1}{G_2R_2}}} > 1 \quad . \tag{C4}$$

Eqn. (C4) is the arrest condition at point H while eqn. (C3) is the arrest condition at point C, where it is emphasized that in this discussion point C is within the arrester section. The dependence of eqns. (C3) and (C4) is of interest.

If the crack is not arrested at H, then from eqn. (C4)

$$\frac{1}{\sqrt{n\,\frac{G_1R_1}{G_2R_2}}} \leq 1 \quad . \tag{C5}$$

Thus, the crack proceeds to point C and encounters the arrest condition represented by eqn. (C3). For this case, because eqn. (C5) is known, the crack will not arrest if the right-hand side of eqn. (C3) is equal to or larger than unity. So the crack may be arrested at point C if the right-hand side of eqn. (C3) is less than unity, that is, if

$$\frac{\left[\frac{2}{n} + \frac{\left(1 - \frac{\dot{\ell}_2}{C_2}\right)\left(\frac{C_2}{C_1}\frac{G_1}{G_2} - 1\right)}{\left(1 + \frac{G_1}{G_2}\frac{\dot{\ell}_2}{C_1}\right)}\right]}{\left(\frac{C_2}{C_1}\frac{G_1}{G_2} + 1\right)} < 1 \quad . \tag{C6}$$

The crack velocity $\dot{\ell}_2$ is permitted to be non-negative. The left-hand side of eqn. (C6) will be maximized by letting $\dot{\ell}_2 = 0$. Thus, expression (C6) will certainly hold if the following condition is satisfied:

$$\frac{\frac{2}{n} + \left(\frac{C_2}{C_1}\frac{G_1}{G_2} - 1\right)}{\frac{C_2}{C_1}\frac{G_1}{G_2} + 1} < 1 \quad . \tag{C7}$$

Expression (C7) can be simplified to

$$\frac{2}{n} + \frac{C_2}{C_1}\frac{G_1}{G_2} - 1 < \frac{C_2}{C_1}\frac{G_1}{G_2} + 1$$

or,

$$\frac{1}{n} < 1 \quad . \tag{C8}$$

The condition (C8) is always valid because n is always greater than unity, and so expression (C6) will always hold.

Thus, the right-hand side of expression (C3) is less than unity and so the condition (C3) is less stringent than the condition (C4). Therefore, if the crack is not arrested as it enters the arrester section, it may arrest within the arrester section at the point where the reflected initial disturbance catches the crack tip.

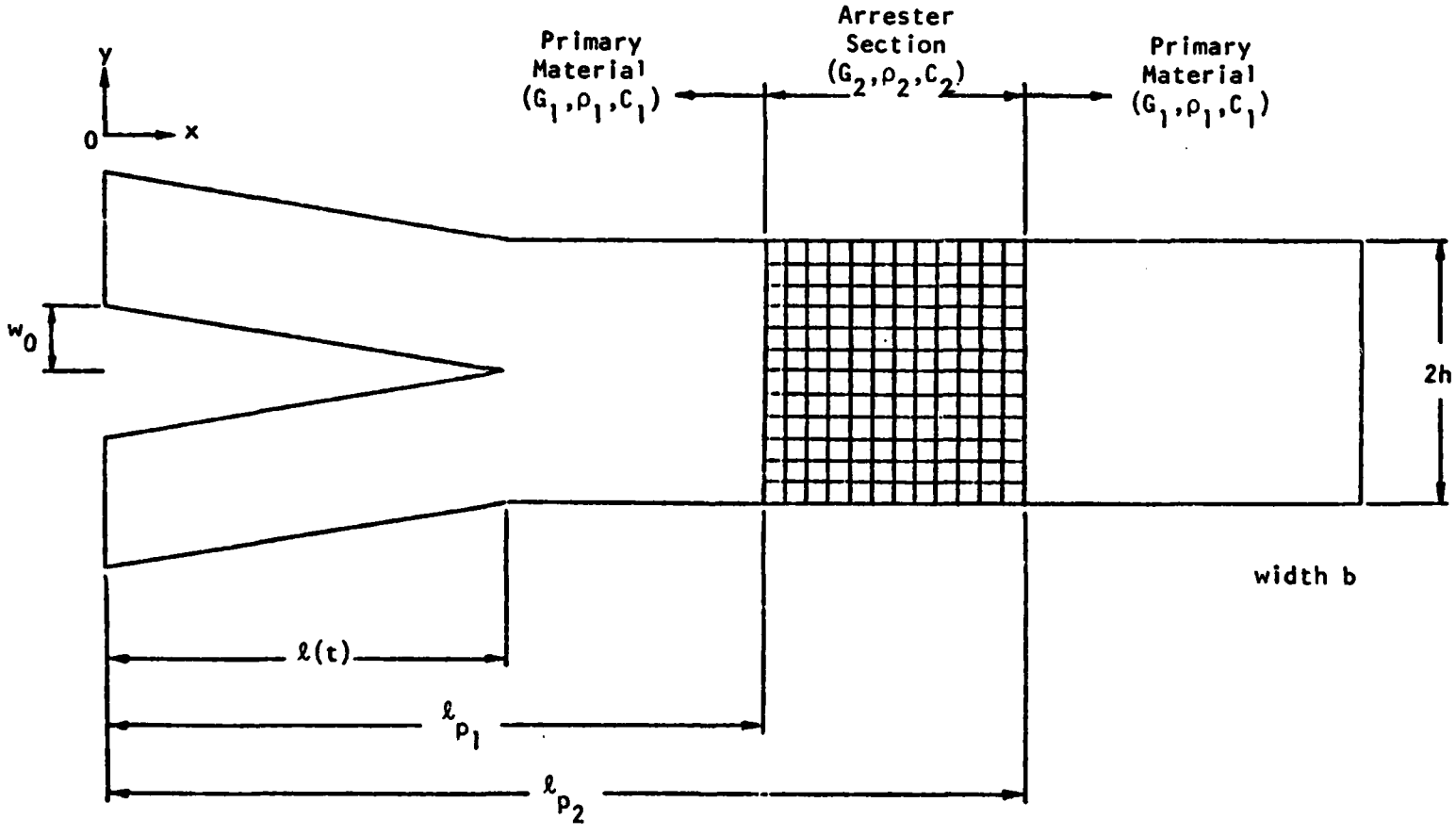

Fig. 1. Double cantilever shear beam specimen containing a finite width arrester section.

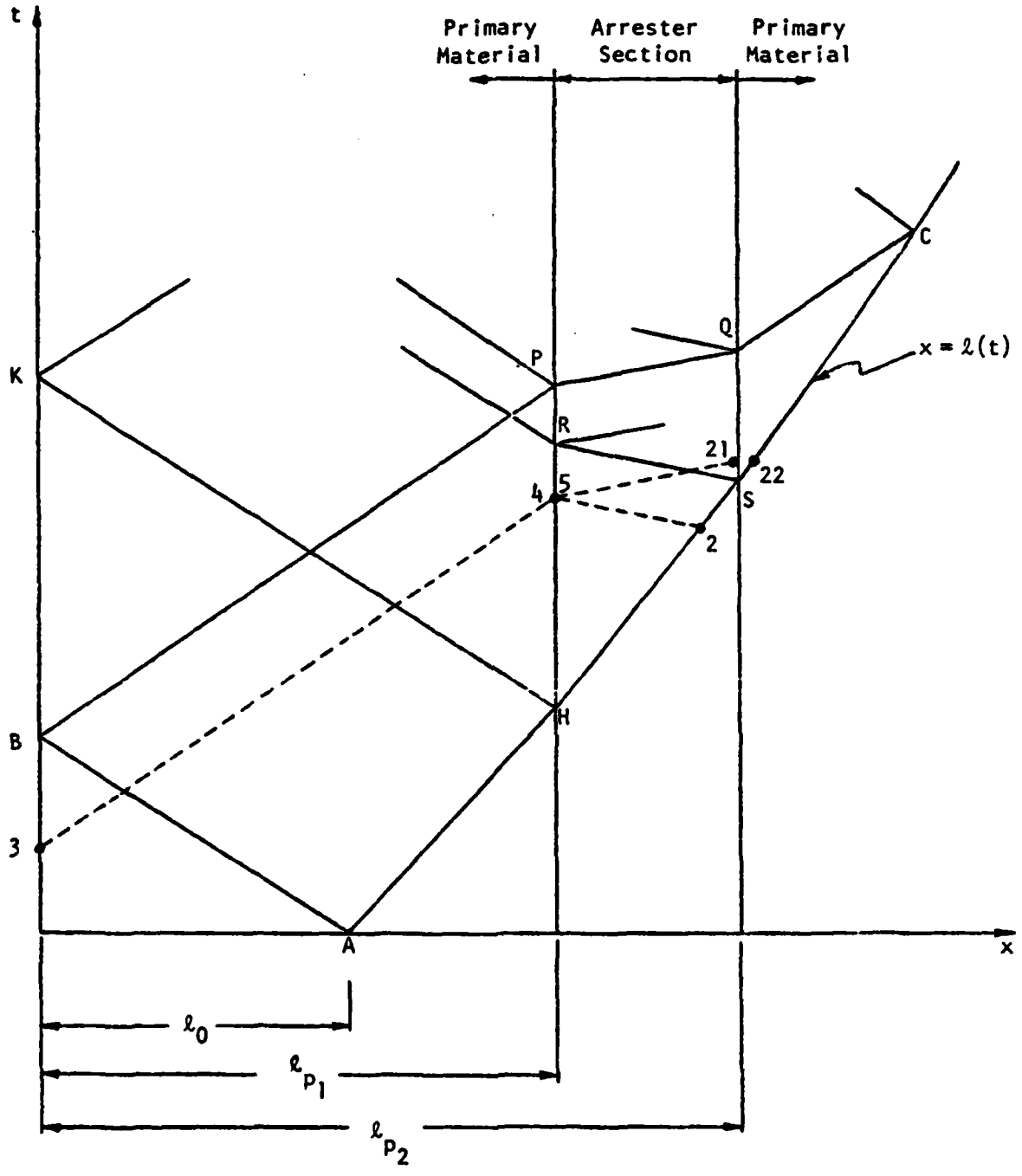

Fig. 2. The (x,t) plane showing the crack-tip trajectory and certain characteristic lines for evaluating the crack-tip conditions at point 22.

END

DTIC

5-86

END

DTIC

5-86